◇ Monograph Excerpt ◇

Matter Antimatter Fluctuations

search, discovery and analysis of Bs flavor oscillations

Nuno Leonardo

Complete work published as:
Analysis of B_s oscillations at CDF, MIT Thesis (2006)
Matter antimatter fluctuations, Monograph, LAP Lambert (2011)

Chapter 8

Search for B_s oscillations

The flavor taggers are here applied to the B_s samples and an initial search for the oscillation frequency Δm_s is performed using an amplitude scanning method. A blind analysis approach is adopted.

8.1 Fitting technique

The unbinned maximum likelihood fitting framework is developed and described in previous chapters. The likelihood model presented in the context of the measurement of B^0 flavor oscillations in Chapter 7 serves as the basis also for the study of mixing in the B_s system, in the partially $D_s l$ and the fully $D_s\pi(\pi\pi)$ reconstructed modes.

The fit input quantities are, for the individual B_s candidates, the following: mass m, proper decay time t, proper decay time uncertainty σ_t, tagging decision ξ, and tagging dilution $\mathcal{D}$. Each sample component α is modeled in the spaces of these input variables through corresponding likelihood factors $\mathcal{P}$, which are evaluated for each candidate i and combined to form the likelihood function $\mathcal{L}$ which is to be maximized in the fitting process,

$$\mathcal{L} = \prod_i \sum_\alpha f_\alpha \mathcal{P}_i^\alpha \qquad \text{with} \qquad \mathcal{P} = L_m \, L_t \, L_\xi \, L_\mathcal{D} \, L_{\sigma_t}.$$

The likelihood factors L_{σ_t} and $L_\mathcal{D}$ do not themselves contain fit parameters and are realized by distributions obtained from the data sample being fit (Section 7.1). The mass PDF L_m was described in Section 5.4 for the various B_s sample components. The likelihood models for proper decay time L_t and flavor tagging L_ξ follow a general description consonant with that given in Chapter 7 for the $B^{+,0}$ samples. However, a few outstanding differences arise, which are addressed in the following sections. The introduction of the amplitude, which is the primary fitting parameter of interest, is the most prominent difference. It

appears as part of the description of the signal components, and arises in the implementation of the fitting method used for the study of the rapid time-dependent flavor oscillations which characterize the B_s system.

8.2 Flavor tagging and input calibration

The leading factors determining the significance of a B_s oscillating signal, besides the data samples size and purity, are the flavor tagging performance and the proper decay time resolution. The calibration of these fit input quantities, accomplished in previous chapters, is thus crucial.

In this chapter, the b-flavor information is provided by the opposite-side tagging methods only. An exclusive combination of those methods is used, as explained in Section 7.2, such that for a B_s candidate which is non-trivially tagged by several algorithms the elected tagging decision is that provided by the algorithm with the highest average dilution. The tagging algorithm raw dilutions are evaluated for each candidate according to the dependencies on event properties presented in Chapter 6. Further calibration of such dilution parameterizations is achieved in the mixing and tagging studies undertaken in Chapter 7. We implement therefore the re-scaling of the dilutions for each of the tagging algorithms,

$$\mathcal{D}_j \;\; \mapsto \;\; S_j \cdot \mathcal{D}_j \; , \tag{8.1}$$

according to the overall dilution scale factors $\{S_i\}$ shown in Table 7.2. Specifically, the factors applied to the $D_s\pi(\pi\pi)$ and $D_s l$ modes are those found for the kinematically similar hadronic and semileptonic $B^{+,0}$ samples, respectively.

The raw proper decay time uncertainty σ_t returned by the vertex fitter is in general underestimated as described in Chapter 5. A detailed calibration procedure is implemented in Section 5.7. The re-scaling of this fit input quantity is thus achieved,

$$\sigma_t \;\; \mapsto \;\; S_t \cdot \sigma_t \; , \tag{8.2}$$

on a per-event basis, through the scale factor parameterizations (5.36) explored in Section 5.7 which take into account dependencies on topological and kinematical vertex characteristics.

8.3 Amplitude method

The analysis method which we employ for the study of flavor oscillations in the B_s system is distinct from that used in the B^0 system in that the oscillation frequency Δm_s is not directly determined as a parameter of the fit.

Such an alternative method is motivated by the B_s mixing frequency being expected to be at least ~ 30 times larger than Δm_d, and that therefore the corresponding time-dependent oscillation patterns may not be adequately discernible with our present sample size and effective resolution for a direct observation to be feasible.

The amplitude method [33] used for probing flavor oscillations in the B_s system is based on the introduction of a Fourier-like coefficient, the amplitude $\mathcal{A}$, multiplying the cosine modulation term in the signal model,

$$1 \pm \cos(wt) \;\; \mapsto \;\; 1 \pm \mathcal{A} \cdot \cos(wt) \; . \tag{8.3}$$

By fixing the oscillation frequency to a given test value, the fit result for the parameter $\mathcal{A}$ is expected to be unit in case the probed frequency coincides with the true oscillation frequency of the system, $w = \Delta m_s$, and be zero otherwise. The execution of this method involves performing a scan in w and a measurement of the amplitude at each value. The output of the procedure is accordingly a list of fitted values $\{\mathcal{A}, \sigma_{\mathcal{A}}\}$ obtained for each probed frequency.

An analysis is said to have sensitivity in a given frequency range if the expected uncertainty on the measured amplitudes is small enough compared to unity, so that the two values $\mathcal{A} = 1$ and $\mathcal{A} = 0$ may be distinguished. The sensitivity of the analysis is here defined as the value of the frequency w for which a measured null amplitude value $\mathcal{A} = 0$ would imply the exclusion of $\mathcal{A} = 1$ at the desired confidence level. The degree of exclusion of a given frequency in the scan, for which the measured amplitude and associated uncertainty are $\mathcal{A}$ and $\sigma_{\mathcal{A}}$, is given by

$$\frac{1}{\sqrt{2\pi}\,\sigma_{\mathcal{A}}} \int_{-\infty}^{1} e^{-\frac{(x-\mathcal{A})^2}{2\,\sigma_{\mathcal{A}}^2}} \; dx \; . \tag{8.4}$$

Specifically, for a confidence level of 95%, which is nominally used, the exclusion and sensitivity conditions are expressed accordingly as follows:

$$\begin{aligned} \mathcal{A} + 1.645 \cdot \sigma_{\mathcal{A}} \;\; &< 1 \qquad 95\%\,\text{C.L. exclusion condition}\,, \\ 1.645 \cdot \sigma_{\mathcal{A}} \;\; &= 1 \qquad 95\%\,\text{C.L. sensitivity condition}\,. \end{aligned}$$

The exclusion *limit* is defined as the largest frequency value below which all frequencies are excluded.

A notable advantage of the indirect probe for oscillations offered by the method stems from the fact that the dependence on $\mathcal{A}$ is linear (8.3). The measurement of $\mathcal{A}$ is hence Gaussian (8.4), and the issue of merging different experimental measurements is straightforward. In effect, the amplitude results obtained at a given frequency point by two experiments

(labeled 1 and 2) may be combined [33],

$$\mathcal{A} = \left(\frac{\mathcal{A}_1}{\sigma^2_{\mathcal{A},1}} + \frac{\mathcal{A}_2}{\sigma^2_{\mathcal{A},2}} \right) \cdot \sigma^2_{\mathcal{A}} \qquad \text{with} \qquad \frac{1}{\sigma^2_{\mathcal{A}}} = \frac{1}{\sigma^2_{\mathcal{A},1}} + \frac{1}{\sigma^2_{\mathcal{A},2}} \,, \tag{8.5}$$

as independent measurements of a same physics quantity.

8.4 Likelihood description

We review in this section the likelihood description for the various sample components. The characterization of the samples accomplished in Chapter 5 is independent of flavor information. The treatment of the latter is achieved in Chapter 7. In the following we thus concentrate mostly on tagging and mixing related aspects which are specific to the B_s samples.

The mixing PDF for signal components, taking into consideration the description of tagging, proper time resolution, t-biasing effects, and partial reconstruction, has been previously derived (7.17). With the introduction of the amplitude parameter (8.3), the PDF takes the following form,

$$\begin{aligned} & L_{t,\xi}(t, \xi_j | \mathcal{A}; \mathcal{D}_j, \{\epsilon_i\}, w, \tau, \sigma_t) \qquad (8.6) \\ & = \begin{cases} (1 - \sum_i \epsilon_i) \, \frac{1}{\mathcal{N}} \frac{1}{\tau} e^{-\frac{t}{\tau}} \theta(t) \otimes_\kappa \mathcal{F}(\kappa) \otimes G(t; \sigma_t) \cdot \mathcal{E}(t) & \text{for} \quad \forall_i \, \xi_i = \ \ 0 \,, \\ \epsilon_j \frac{1 - \mathcal{D}_j \mathcal{A} \cos(wt)}{2} \, \frac{1}{\mathcal{N}} \frac{1}{\tau} e^{-\frac{t}{\tau}} \theta(t) \otimes_\kappa \mathcal{F}(\kappa) \otimes G(t; \sigma_t) \cdot \mathcal{E}(t) & \text{for} \quad \xi_j = -1 \,, \\ \epsilon_j \frac{1 + \mathcal{D}_j \mathcal{A} \cos(wt)}{2} \, \frac{1}{\mathcal{N}} \frac{1}{\tau} e^{-\frac{t}{\tau}} \theta(t) \otimes_\kappa \mathcal{F}(\kappa) \otimes G(t; \sigma_t) \cdot \mathcal{E}(t) & \text{for} \quad \xi_j = +1 \,, \end{cases} \\ & = \ p_{\{\epsilon_i\}}(\xi_j) \cdot \frac{1}{\mathcal{N}} \, \frac{E(t;\tau) + \xi_j \mathcal{D}_j \, \mathcal{A} \, C(t; \tau, w)}{1 + |\xi_j|} \otimes_\kappa \mathcal{F}(\kappa) \otimes G(t; \sigma_t) \cdot \mathcal{E}(t) \,. \end{aligned}$$

The parameter w takes on the value of the oscillation frequency being probed. The j-index is used to indicate the algorithm employed for tagging the event, the efficiency factor $p_{\{\epsilon_i\}}$ being given by (7.16). The proper decay time resolution function $G(t; \sigma_t)$ is defined in (5.14), and the t-efficiency function $\mathcal{E}(t)$ in Section 5.3.1. For the semileptonic modes, the effects of partial reconstruction are described through smearing with the κ-factor distribution $\mathcal{F}(\kappa)$ addressed in Section 5.3.2. Such effects are not present in the fully reconstructed modes, which formally corresponds to imposing $\mathcal{F}(\kappa) = \delta(\kappa - 1)$. The definitions of the functions E

and C are tacitly implied by the second equality in the equation. The normalization constant $\mathcal{N}$ is given in (5.20) and (5.23).

From (8.6), the importance of the taggers calibration expressed in (8.1) becomes apparent. It readily shows that the introduction of the amplitude parameter forbids the possibility of simultaneously extracting the tagging dilution which it directly multiplies. In fact, the determination of the main parameter of interest, $\mathcal{A}$, requires thus the accurate knowledge of the dilution, which justifies the necessity of previously accomplishing its calibration.

For non-physics background components, the tagging predicted dilutions $\mathcal{D}_j$ have no particular meaning, thus not being used in the corresponding PDFs. The latter contain instead terms which account for possible background flavor asymmetries which are globally described by dilution-like fit *parameters*, D_j. For such components, where mixing effects are not considered, the descriptions of proper decay time and tagging are decoupled. Namely, the following model is used

$$L_{t,\xi}(t,\xi|D_j,\{\epsilon_i\}) \;=\; p_{\{\epsilon_i\}}(\xi_j)\,\frac{1+\xi_j D_j}{1+|\xi_j|}\;\cdot\; L_t(t)\;. \tag{8.7}$$

The j-index denotes the tagging algorithm providing the decision for the event of which the likelihood is being evaluated. A specific set of fit parameters $\{\epsilon_i, D_i\}$ accounts for tagging related effects. The proper decay time PDF L_t coincides with that presented in Section 5.2 for the relevant background components. Specifically, the model expressed by (8.7) is employed for the combinatorial background in all samples, as well as the fakes background in the semileptonic samples.

In general, an identical model as used for signal (8.6) is employed for the physics backgrounds as well. Specifically, for the $D_s\pi(\pi\pi)$, the Cabibbo-suppressed, the exclusively and partially reconstructed B_s background modes all share the same model and parameters employed for the signal component.

A full signal-like treatment is devoted to the partially reconstructed physics backgrounds in the $D_s l$ samples. That is, a model identical to that of the nominal signal (8.6) is employed to describe the contributions coming from the involved additional B_α (with $\alpha = u, d, s$) decays,

$$\begin{aligned} &L^{\alpha}_{t,\xi}(t,\xi_j|\lambda_\alpha;\mathcal{D}_j,\{\epsilon_i\},w_\alpha,\tau_\alpha,\sigma_t) \\ &=\; p_{\{\epsilon_i\}}(\xi_j)\cdot\frac{1}{\mathcal{N}_\alpha}\,\frac{E(t;\tau_\alpha)+\xi_j\mathcal{D}_j\;\lambda_\alpha\;C(t;\tau_\alpha,w_\alpha)}{1+|\xi_j|}\otimes_\kappa\mathcal{F}_\alpha(\kappa)\otimes G(t;\sigma_t)\cdot\mathcal{E}_\alpha(t)\;, \end{aligned} \tag{8.8}$$

where $\lambda_u = \lambda_d = 1$, and $\lambda_s = \mathcal{A}$; $w_u = 0$, $w_d = \Delta m_d$, and w_s stands for the Δm_s hypothesis. The tagging efficiency parameters $\{\epsilon_i\}$ are identified with those associated to the signal component in (8.6). The parameters τ_u, τ_d, and τ_u correspond to the B^+, B^0, and B_s mesons

lifetimes, respectively. Specific κ-factor distributions $\mathcal{F}_\alpha(\kappa)$, and t-efficiency functions $\mathcal{E}_\alpha(t)$ are derived from Monte Carlo simulation of the contributing decays to each component.

8.5 Fits of the blinded data

The fits to the data samples are performed first with the true tagging information provisionally *hidden*. A *blinding* strategy in data analysis, generally speaking, implies avoiding knowing the final answer of the measurement until the procedure is fully specified and carried out. We adopt such a strategy which allows nevertheless for the full characterization of the samples to be achieved, except for the main quantity of interest, $\mathcal{A}$, along with the background flavor asymmetries. The analysis is fully performed in this fashion. Next, in Section 8.6, the systematic uncertainties are evaluated and, finally, the amplitude fits are repeated with the *unblinded* tagging input, in Section 8.7.

The tagging decision at input to the fitter is multiplied by the factor $(-1)^n$, with n standing for an integer specifying the event's ordering and thus being completely unconnected to tagging information. This scrambling of the tagging decisions thus hides the effects of a potential oscillation signal in the probed frequency region, and forbids that any interpretation be made from the central values of the fitted amplitude. We note, nevertheless, that the tagging status $\xi = 0$ and $\xi \neq 0$ are not confused by the scrambling criteria, and that thus the fractions of each such class of candidates for each tagging method remains unaffected. This way the taggers' efficiencies may be determined from the fits. The tagging dilutions are provided to the fit as input with no modification. The procedure allows accordingly for the determination of the uncertainty on the amplitude $\sigma_{\mathcal{A}}$, for each probed frequency, and therefore the sensitivity of the fitted samples is inferred.

The determination of the main parameter of interest, the amplitude, is performed once all other fit parameters have been found and thereafter fixed. The model parameters describing the mass and proper decay time spaces for the B_s samples are obtained in the fits to the data performed in Chapter 5 in the absence of flavor information. The parameters which remain to be determined depend on the flavor taggers' information, and correspond to:

1. the taggers' efficiencies $\{\epsilon_i\}$ for backgrounds and signal components,

2. the flavor asymmetries $\{D_i\}$ of non-physics backgrounds for each tagger,

3. the amplitude, $\mathcal{A}$, for each fixed value of the oscillation frequency, w for Δm_s.

Fits are first performed to the individual samples for the tagging efficiency and the flavor asymmetry parameters of the non-physics backgrounds. Those describing the combinatorial

backgrounds are found from fits to the mass-sideband candidates. For the fakes background in the semileptonic modes, tagging asymmetries are imposed to be null, and the efficiency parameters are commonly identified with those to be determined for the signal components. A combined fit is then performed to the hadronic samples, as well as to the semileptonic ones. The efficiency parameters are thus found, commonly for either the hadronic or the semileptonic samples, which are associated to the signal and physics-background sample components.

The final stage of the fitting procedure corresponds to the amplitude fits. Here the amplitude parameter is the only free parameter floating, to be adjusted in the likelihood maximization, all other parameters being fixed to the values formerly determined. The amplitude is a common parameter in the fits performed simultaneously to all sub-samples of the fully, and of the partially reconstructed modes. The frequency region $(0, 20)$ [ps^{-1}] is discretized in steps of 0.25 ps^{-1}, and the amplitude fit is repeated at each such fixed frequency value. The scan results correspond thus to the sequence of measured pair values $(\mathcal{A}, \sigma_{\mathcal{A}})$, of the fitted amplitude and associated uncertainty, for each Δm_s hypothesis.

The results of the blinded amplitude scans are shown in Figures 8.1 and 8.2 for the combined $D_s\pi(\pi\pi)$ and $D_s l$ samples, respectively. We note that the amplitude uncertainties shown are statistical only. Technically, in fact, while asymmetric uncertainties are provided by the likelihood minimization in fitting, only the upper uncertainties are used.

Although exclusion conditions, which do depend on the central fitted values, cannot be inferred from these blinded results, several assertions can be drawn. Similar statistical sensitivities are observed for the hadronic and semileptonic samples, of approximately 11 ps^{-1}. However such value alone hides in fact the rather distinct observed behavior in the two scans at lower and higher frequencies, which are predominantly determined by the samples' statistics and resolutions, respectively. As expected, thus, the amplitude uncertainties in the lower region of the spectrum are considerably smaller in the semileptonic scan than in the hadronic, while the reverse is true for the upper frequency region. This relative complementarity of the two classes of B_s samples will result in a considerable improved behavior in the combined amplitude scan.

8.6 Systematic uncertainties

Method of evaluation

A few issues arise regarding the estimation of systematic uncertainties on the amplitude parameter. For the purpose of establishing exclusion conditions for a given Δm_s hypothesis,

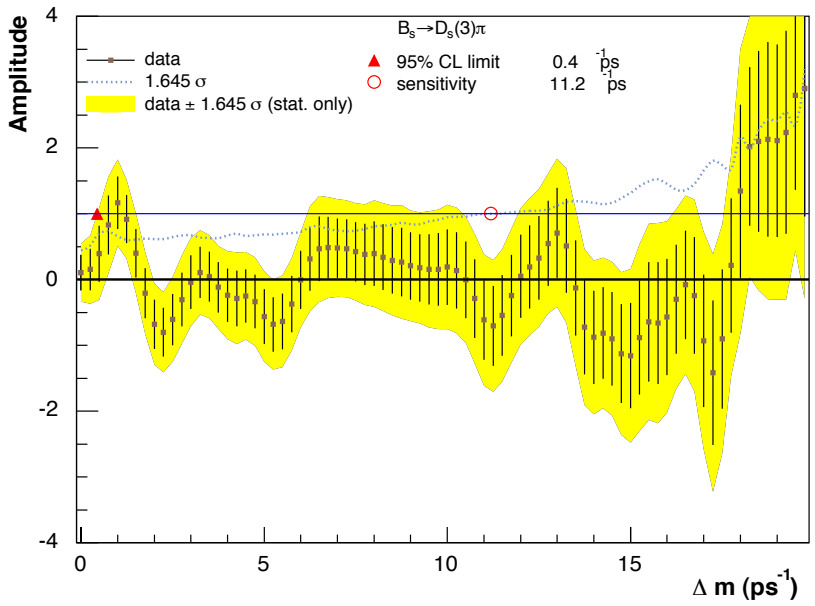

Figure 8.1: Blinded amplitude scan for $D_s\pi(\pi\pi)$ samples; uncertainties are statistical only.

both the corresponding fitted amplitude value and its uncertainty are directly employed. The point to emphasize is that systematic induced changes in the amplitude and in the statistical uncertainty on the amplitude, at a given frequency point in the scan, are correlated. The adequate evaluation of systematic uncertainties is derived in [33] and is expressed as

$$\sigma_{\mathcal{A}}^{\text{syst}} \;=\; \Delta\mathcal{A} + (1-\mathcal{A})\,\frac{\Delta\,\sigma_{\mathcal{A}}}{\sigma_{\mathcal{A}}}\,, \tag{8.9}$$

where $\Delta\mathcal{A}$ and $\Delta\,\sigma_{\mathcal{A}}$ are the observed variations in the fitted values for the amplitude and its statistical uncertainty induced by the systematic effect, relative to the values obtained in the nominal fit configuration, $\mathcal{A}$ and $\sigma_{\mathcal{A}}$.

The evaluation of the systematic uncertainties is fully based on toy Monte Carlo simulation. The latter provides a reliable parametric description of the fit input data, consistent with the likelihood models employed for each sample component. The parameters are set to those values previously found in fits to the data in Section 8.5. The toy Monte Carlo is generated with the value of the mixing frequency Δm_s for which the systematic uncertainty is to be evaluated. It is in effect this latter requirement of correspondence between the point of the amplitude scan and the true Δm_s value that has lead to the use of the toy Monte Carlo exclusively based approach to systematics evaluation. The toy Monte Carlo samples contain comparable statistics to the data samples, in order to get distributions of returned amplitudes and uncertainties representative of those which would be expected in the data.

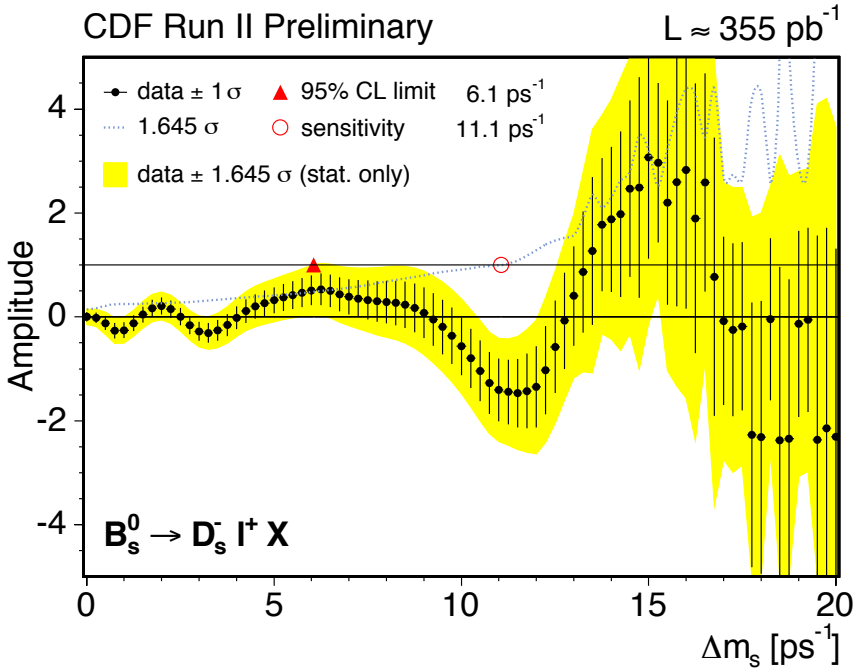

Figure 8.2: Blinded amplitude scan for $D_s l$ samples; uncertainties are statistical only.

For each source of systematic uncertainty considered, a large set of about $1,000$ toy Monte Carlo samples is generated at each Δm_s value. Each of these samples is then fit under the nominal conditions, giving fit results $(\mathcal{A}^0, \sigma^0_{\mathcal{A}})$, and again with the variation on the systematic effect incorporated, with results $(\mathcal{A}^1, \sigma^1_{\mathcal{A}})$. The following quantity, analogous to (8.9), is then formed for each sample (i),

$$(\sigma^{\rm syst}_{\mathcal{A}})^i = (\mathcal{A}^1 - \mathcal{A}^0) + (1 - \mathcal{A}^0)\,\frac{\sigma^1_{\mathcal{A}} - \sigma^0_{\mathcal{A}}}{\sigma^0_{\mathcal{A}}}\ , \tag{8.10}$$

and its distribution is prepared for each samples' ensemble. The uncertainty contribution from each systematics source, at a given frequency point, is obtained as the mean of the above distribution, in case the systematic variation corresponds to turning an effect on or off, or to step-wise parameter variations. For a continuous variation, when parameter values are modified according to a distribution, the corresponding systematic contribution corresponds to the width of the distribution obtained from (8.10).

The systematic uncertainties evaluation procedure is repeated at a number of Δm_s values sampled in the probed frequency range. The contributions from the various systematics sources obtained at each such frequency point are added in quadrature. The outcome is then a profile $\sigma_{\mathcal{A}}(\Delta m_s)$ which is interpolated to give the systematic uncertainties for all frequency points in the scan. These are combined in quadrature to the statistical uncertainty on the

amplitude obtained from the nominal fit. The exclusion condition, derived in Section 8.3, for a given probed frequency point $w = \Delta m_s$ becomes

$$\mathcal{A}(w) + 1.645\sqrt{\sigma_{\mathcal{A}}(w)^2 + \sigma_{\mathcal{A}}^{\text{syst}}(w)^2} < 1 \; .$$

Uncertainty sources

Systematic uncertainties on the amplitude parameter are evaluated for the following sources.

Physics background levels: The amounts of physics backgrounds are known only to limited precision. In general, variations of the corresponding fraction parameters are implemented within uncertainties. For the Cabibbo-suppressed $B_s \to D_s K(\pi\pi)$ modes relative fraction uncertainties of 50% are assigned. The contribution from the partially reconstructed decays in the hadronic samples is nominally fixed to the Monte Carlo estimation. Variations are implemented where mass template parameters are allowed to float.

Semileptonic signal composition: The branching fractions of inclusive B_s decays to $D_s l$ and $D_s^{*(*)} l$ are not well known. The ratio of branching fractions for these contributions is varied by 20%. The κ-factor distributions and t-efficiency functions are modified accordingly as well.

Non-physics backgrounds in semileptonic samples: The fractions and shapes of the fakes background contributions are obtained respectively from fits to the fakes lepton samples and to the $m_{D_s l}$ distributions. Variations within the statistic uncertainties obtained from those fits are imposed as systematic effects. For the combinatorial background parameter variations are induced by extending the D_s mass-sideband regions by ± 50 MeV/c^2.

Dilution of fakes background in semileptonic samples: A null flavor asymmetry is assigned to the fakes background in the nominal fit. Variations of these dilution background parameters are taken within the dilution input values for signal.

Dilution and proper time uncertainty input calibration: Variations of the scale factors used for dilution (8.1) and proper decay time (8.2) calibration are taken in accordance with the values quoted in Tables 7.2 and 5.14, respectively.

Dilution and proper time uncertainty templates: The likelihood factors $L_{\mathcal{D}}$ and L_{σ_t} normally correspond to distributions obtained from sideband and sideband-subtracted data. The limited sample sizes and tagging efficiencies imply that some of these distributions may not be adequately populated. Variations of the dilution templates are constructed by continuously modifying the bin contents, through Gaussian-smearing, according to their statistical uncertainties. For the $D_s\pi(\pi\pi)$ samples, uniform templates are employed for the L_{σ_t} factors in the nominal fits. The resulting systematic effects are estimated by including non-trivial templates in the fits to the toy Monte Carlo.

Construction of t-efficiency curves, $\mathcal{E}(t)$: The t-efficiency functions are constructed from realistic Monte Carlo simulation, and small modifications may thus be induced by simulation related effects. The procedure used for evaluation of corresponding systematic shifts is similar to that described in Section 7.6. These correspond to relatively small contributions, which are neglected for the hadronic modes.

Unaccounted mixing effects in physics backgrounds: A full signal-like description (8.8) of the physics backgrounds is implemented for the semileptonic samples. For the hadronic samples, however, mixing effects are not considered in the models employed for the partially reconstructed B_s and misreconstructed B^0 contributions. No flavor asymmetry is assigned to these. Variations are estimated by incorporating oscillations, at the corresponding frequencies, in the toy Monte Carlo simulation.

Non-negligible $\Delta\Gamma/\Gamma$: The derivation of the proper decay time model in mixing used in the nominal fits are made in the assumption of zero lifetime difference between the two B_s mass eigenstates. In the case of a non-negligible lifetime difference, contributions corresponding to the two $\Gamma = 1/\tau$ values are introduced (2.18) in the signal model. Its effect is evaluated by modifying the Monte Carlo generation model. A value of $\Delta\Gamma/\Gamma = 0.2$ is used in the simulation.

Resolution model: The detector resolution of the proper decay time is nominally modeled through a single Gaussian function (5.14). The effect of more elaborate resolution models is evaluated by fitting Monte Carlo samples generated with models involving an additional Gaussian and an exponential function. Specifically, the former is characterized by a width of $2.5\,\sigma_t$ and a fraction of 17%, and the latter by a decay constant of about 100 μm and 1% fraction.

Summary of uncertainty results

The evaluated contributions from systematic sources discussed above for the fully and the partially reconstructed combined samples are compiled in Tables 8.1 and 8.2, respectively, for selected frequency points in the amplitude scan. The dominant contributions are the dilution scale factors, for the hadronic modes, and the level of physics backgrounds in the semileptonic samples. A graphical representation of the variation of each such contribution with Δm_s, obtained through polynomial interpolation, is presented in Figures 8.3 and 8.4. The uppermost curve corresponds to the combined systematic uncertainties for each case.

We point out that the evaluated systematic uncertainties on the amplitude are considerably smaller than the corresponding statistical uncertainties. We note also that with increasing sample sizes the dominant systematic sources will be also better controlled, and are thus not expected to impose precision limitations.

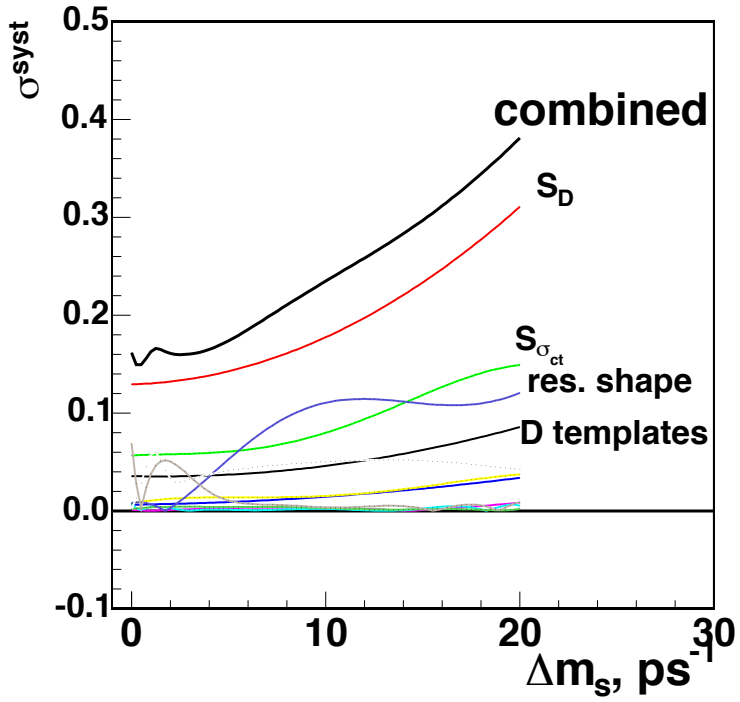

Figure 8.3: Summary graph of systematic uncertainties in the hadronic scan.

source	uncertainty at selected frequency point				
	0 ps^{-1}	5 ps^{-1}	10 ps^{-1}	15 ps^{-1}	20 ps^{-1}
physics background level	0.069	0.020	0.002	0.034	0.005
σ_{ct} scale factor	0.057	0.061	0.080	0.118	0.149
σ_{ct} templates	0.001	0.003	0.003	0.001	0.008
dilution scale factors	0.129	0.143	0.177	0.233	0.311
dilution templates	0.036	0.037	0.046	0.062	0.086
mixing in physics background	0.008	0.004	0.004	0.003	0.006
non-negligible $\Delta\Gamma/\Gamma$	0.002	0.041	0.050	0.051	0.043
resolution model	0.008	0.053	0.110	0.110	0.120
total systematic uncertainty	0.162	0.174	0.235	0.297	0.381
statistical uncertainty	0.251	0.400	0.567	0.846	1.177

Table 8.1: Summary of the uncertainties on the amplitude at selected frequency points in the hadronic scan.

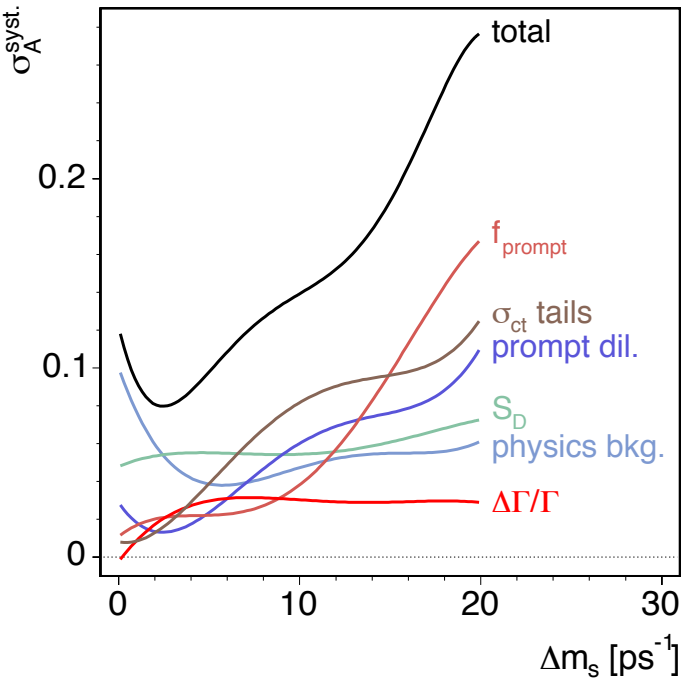

Figure 8.4: Summary graph of systematic uncertainties in the semileptonic scan.

source	uncertainty at selected frequency point				
	0 ps^{-1}	5 ps^{-1}	10 ps^{-1}	15 ps^{-1}	20 ps^{-1}
physics background level	0.107	0.041	0.044	0.054	0.060
fakes background level	0.012	0.024	0.042	0.102	0.177
combinatorial background level	0.011	0.021	0.029	0.036	0.042
signal composition	0.002	0.004	0.005	0.006	0.010
t-efficiency function	0.001	0.006	0.015	0.021	0.035
σ_t scale factor	0.001	0.019	0.024	0.030	0.070
dilution scale factors	0.047	0.054	0.054	0.061	0.073
fakes background dilution	0.036	0.027	0.057	0.075	0.109
non-negligible $\Delta\Gamma/\Gamma$	0.001	0.029	0.031	0.029	0.029
resolution model	0.006	0.031	0.080	0.094	0.125
total systematic uncertainty	0.123	0.093	0.138	0.187	0.277
statistical	0.088	0.252	0.565	0.758	1.850

Table 8.2: Summary of the uncertainties on the amplitude at selected frequency points in the semileptonic scan.

8.7 Results

The final step of the analysis, after having fully established the systematic uncertainties and the sensitivity of the measurements on the blinded samples, is to repeat the amplitude scans by removing the randomization of the tagging decision. The results of these unblinded amplitude scans are shown in Figures 8.5 and 8.6 for the fully and partially reconstructed B_s samples, respectively. The 95% exclusion limits obtained separately with the hadronic and semileptonic modes are 9.8 ps^{-1} and 10.4 ps^{-1}, respectively.

The combined analysis results are presented in Figure 8.7 which shows the amplitude scan obtained by combining, using (8.5), the hadronic and the semileptonic amplitude measurements. The uncertainty on the amplitude remains smaller than unity up until 17 ps^{-1}. The 95% sensitivity condition is verified exactly at 13.0 ps^{-1}, and approximately until 17 ps^{-1}, as indicated by the significance curve represented in the scan by the dashed line. The region defined by the set of probed points which are excluded at 95% C.L. is the following,

$$\text{excluded region :} \quad (0.00, 8.50) \cup (10.50, 11.50) \cup (12.50, 16.75) \ \text{ps}^{-1} \ .$$

The 95% exclusion limit achieved is 8.6 ps^{-1}.

The amplitude results obtained in previous experiments are summarized in Table 1.8. The achieved Δm_s sensitivity with our current data samples is competitive with the best single experiment. The combined amplitude scan based on previously published results is shown in Figure 1.6. The 95% C.L. exclusion limit and sensitivity are 14.4 ps^{-1} and 18.2 ps^{-1}, respectively. The modified world average amplitude scan with the inclusion of the amplitude measurements represented in Figure 8.7 is shown in Figure 8.8. The improved 95% C.L. exclusion limit is 16.6 ps^{-1}, and the sensitivity is pushed to 19.6 ps^{-1}. Under the assumption that Δm_s lies within the probed spectrum, all frequency values are excluded at 95% C.L. except for the following double-sided interval

$$\text{allowed region :} \quad (16.6, 20.8) \ \text{ps}^{-1} \ .$$

The impact of the reported results obtained with the current data samples on the world average knowledge of Δm_s is already considerable.

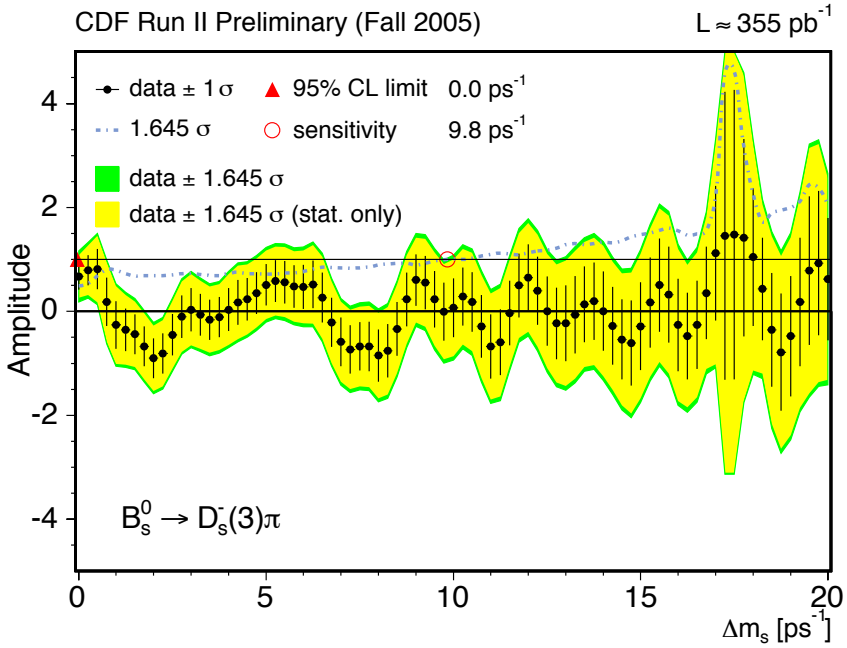

Figure 8.5: Amplitude scan in unblinded data for the hadronic samples.

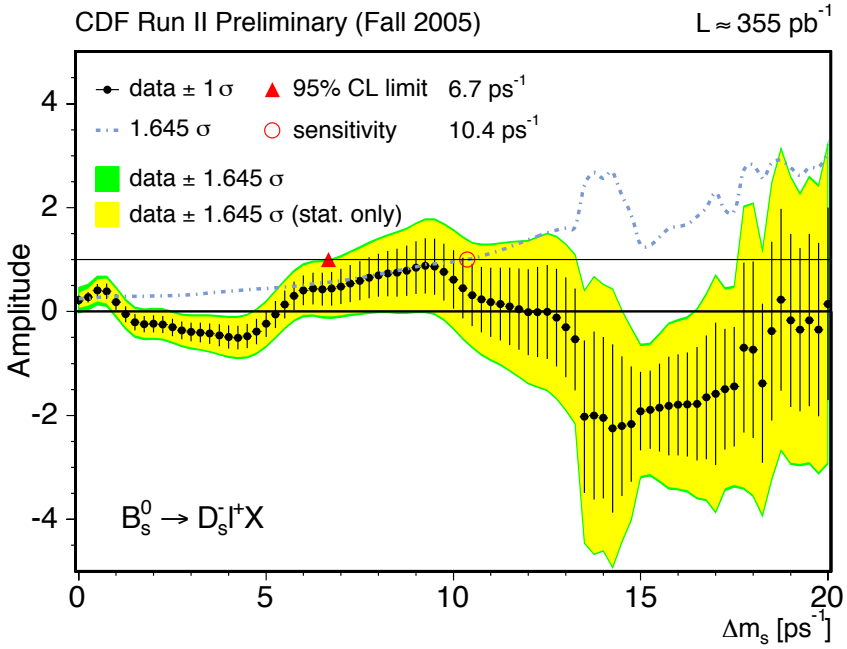

Figure 8.6: Amplitude scan in unblinded data for the semileptonic samples.

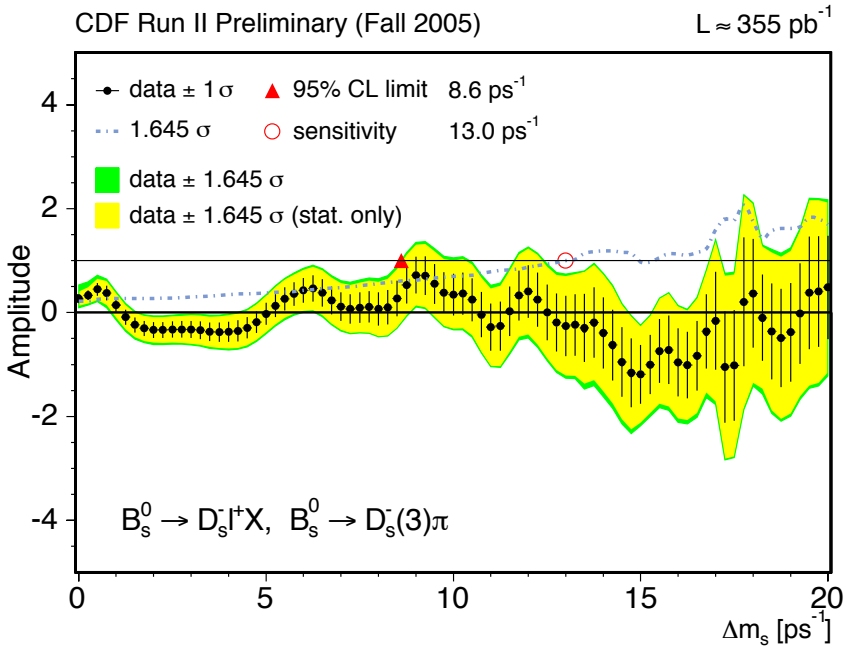

Figure 8.7: Combined amplitude scan in unblinded data for hadronic and semileptonic samples.

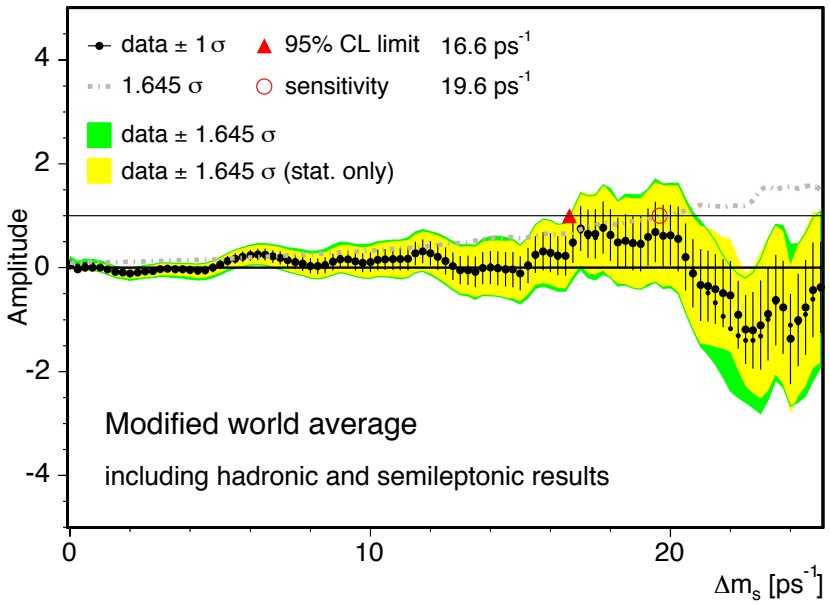

Figure 8.8: Modified world average amplitude scan with hadronic and semileptonic results.

8.8 Résumé

Based on the unbinned fitting framework, likelihood model, flavor tagging, and input calibration previously presented, a search for B_s flavor oscillations was carried out on a $355\,\mathrm{pb}^{-1}$ dataset of fully and partially reconstructed decays. The opposite-side tagging methods presented in Chapter 6 and further calibrated in Chapter 7 are applied to the hadronic $B_s \to D_s\pi(\pi\pi)$ and the semileptonic $B_s \to D_s l X$ decay samples. The underlying samples' description in mass and proper decay time spaces was achieved in Chapter 5, where the calibration of proper decay time uncertainties was also implemented.

In anticipation to the rapid oscillation frequency characterizing the B_s system, an alternative method to the direct determination, as applied for Δm_d in Chapter 7, is employed. The method consists in performing a scan in frequency and measuring at each such frequency value the amplitude of the probed oscillation. This so-called amplitude method, which results appropriate for setting exclusion conditions, essentially combines the utility of a low-statistics resonance search with a procedure allowing for a straightforward combination of independent experimental measurements.

A blinding technique is adopted, which consists of provisionally randomizing the tagging decisions. The full analysis is first performed in this fashion. The systematic uncertainties on the amplitude are evaluated taking into consideration correlated variations of the amplitude value and its statistical uncertainty, using toy Monte Carlo simulation. The dominant contribution to the combined uncertainty is manifestly statistical.

The quantities which are typically defined to characterize the results of the amplitude scan are the 95% C.L. sensitivity and exclusion limit. From the combined semileptonic and hadronic scans, these are given by:

$$\begin{aligned} \text{exclusion limit}: &\quad 8.6\ \mathrm{ps}^{-1} \quad (95\%\ \text{C.L.}) \\ \text{sensitivity}: &\quad 13.0\ \mathrm{ps}^{-1} \quad (95\%\ \text{C.L.}) \end{aligned}$$

These two quantities provide a short, incomplete summary of the results. The amplitude measurements performed at each probe frequency are combined with previously published results, having already a considerable impact on the accumulated knowledge of Δm_s. From such combination, assuming that the B_s oscillation frequency is smaller than $25\ \mathrm{ps}^{-1}$, the interval of frequencies not excluded at 95% C.L. is given by

$$(16.6, 20.8)\ \mathrm{ps}^{-1}\ .$$

The degree of exclusion achieved along the probed frequency spectrum is contained in the full amplitude scan. This complete set of experimental information about Δm_s is what

is employed for all practical purposes, including for constraining the CKM matrix elements which we address in Chapter 12.

The oscillation search was carried out in this chapter, on a part of the full dataset, employing the opposite-side tagging methods alone. In Chapter 9 we present an outstanding improvement in flavor tagging. This addition, with same technique and data sample, will lead to the emergence of the first significant B_s oscillation signal.